International Journal of Electrical and Electronics Engineers
Vol. No. 8, Issue No. 02, July-December 2016
ISSN (O) 2321-2055
ISSN (P) 2321-2045

ROBUST TECHNIQUE FOR IMAGE DENOISING BY COMPONENT PROCESSING USING VTV & PB METHODS

Ashwini R Vidap[1], Vijay Kumar S Kolkure[2]

[1]*E&TC Department, B.M.I.T. Solapur, (India*

[2]*E&TC Department, B.M.I.T. Solapur, India*

ABSTRACT

In this paper, we consider an image decomposition model that provides a novel framework for image denoising. The model computes the components of the image to be processed in a moving frame that encodes its local geometry (directions of gradients and level lines). Then, the strategy we develop is to denoise the components of the image in the moving frame in order to preserve its local geometry, which would have been more affected if processing the image directly. Experiments on a whole image database tested with several denoising methods show that this framework can provide better results than denoising the image directly, both in terms of Peak signal-to-noise ratio and Structural similarity index metrics.In the proposed strategy for denoising, we either combine the components into a single vector-valued function to which we apply a denoising method (VTV) or treat them separately applying the same denoising method but with different parameters (NLM and BM3D).

Keywords: Image Denoising, Local Variational Method, Patch-Based Method, Differential Geometry.

I REVIEW OF DIFFERENT METHODS

Total variation methods[5]

This study proposes a new definition of the total variation norm for vector-valued functions that can be applied to restore color and other vector-valued images. The new TV norm has the desirable properties of 1) not penalizing discontinuities (edges) in the image, 2) being rotationally invariant in the image space, and 3) reducing to the usual TV norm in the scalar case. Some numerical experiments on denoising simple color images in red–green–blue (RGB) color space are presented. We have introduced a new definition of the total variationnorm for vector-valued functions. This definitionhas a number of properties that may be desirable in applications:1) it allows discontinuous functions—edges; 2) it isrotationally invariant in image space; and 3) it reduces to the classical TV norm in the scalar case. We have compared the properties of the norm to other definitions, in particular to the approach of Sapiro [9]. By studying simple examples, i.e., reduction to one dimension in either physical, or color space, we have

illustrated some differences between the norms. A general framework for vector norms was introduced. We find two natural candidates: the TV , and the norms. Of these two, TV does a better job of preserving color transitions. Many promising possible norm definitions fall outside this framework, and are not discussed in this study.

II IMAGE QUALITY ASSESSMENT[10]

This study gives methods for assessing perceptual image quality traditionally attempted to quantify the visibility of errors (differences) between a distorted image and a reference image using a variety of known properties of the human visual system. Under the assumption that human visual perception is highly adapted for extracting structural information from a scene, we introduce an alternative complementary framework for qualityassessment based on the degradation of structural information. As a specific example of this concept, we develop a Structural Similarity Index and demonstrate its promise through a set of intuitive examples, as well as comparison to both subjective ratings and state-of-the-art objective methods on a database of images compressed with JPEG and JPEG2000.1 An image signal whose quality is being evaluated can bethought of as a sum of an undistorted reference signal and anerror signal. A widely adopted assumption is that the loss ofperceptual quality is directly related to the visibility of the errorsignal. The simplest implementation of this concept is the MSE,which objectively quantifies the strength of the error signal. Buttwo distorted images with the same MSE may have very differenttypes of errors, some of which are much more visible thanothers. Most perceptual image quality assessment approachesproposed in the literature attempt to weight different aspects ofthe error signal according to their visibility, as determined bypsychophysical measurements in humans or physiological measurementsin animals.

III HIGHER-ORDER IMAGE STATISTICS[2]

In this study, the restoration of images is an important and widely studied problem in computer vision and image processing. Various image filtering strategies have been effective, but invariably make strong assumptions about the properties of the signal and/or degradation. Therefore, these methods typically lack the generality to be easily applied to new applications or diverse image collections.This paper describes a novel unsupervised, information-theoretic, adaptive filter (UINTA) that improves the predictability of pixel intensities from their neighborhoods by decreasing the joint entropy between them. Thus UINTA automatically discovers the statistical properties of the signal and can thereby restore a wide spectrum of images and applications. This paper describes the formulation required to minimize the joint entropy measure, presents several important practical considerations in estimating image-region statistics, and then presents results on both real and synthetic data.

IV SPINOR FOURIER TRANSFORM[3]

It introduces a new spinor Fourier transform for both gray-level and color image processing. Our approach relies on the three following considerations: mathematically speaking, defining a Fourier transform requires to deal with

group actions; vectors of the acquisition space can be considered as generalized numbers when embedded in aClifford algebra; the tangent space of the image surface appears to be a natural parameter of the transform we define by means of so-called spin characters. The resulting spinor Fourier transform may be used to perform frequency filtering that takes into account the Riemannian geometry of the image.We give examples of low-pass filtering interpretedas diffusion process. When applied to color images, the entire color information is involved in a really non marginal process. The construction involves group actions via spin characters, these ones being parametrized by bivectors of the Clifford algebra. A natural choice for the bivectors is the one corresponding to the tangent planes of the image surface. But other bivectors can be considered.This paper introduces a new approach to orthonormal wavelet image denoising. Instead of postulating a statistical model for the wavelet coefficients, we directly parametrize the denoising process as a sum of elementary nonlinear processes with unknown weights.We then minimize an estimate of the mean square error between the clean image and the denoised one. The key point is that we have at our disposal a very accurate, statistically unbiased, MSE estimate—Stein's unbiased risk estimate that depends on the noisy image alone, not on the clean one. Like the MSE, this estimate is quadratic in the unknown weights, and its minimization amounts to solving a linear system of equations. The existence of this *a priori* estimate makes it unnecessary to devise a specific statistical model for the wavelet coefficients. Instead, and contrary to the custom in the literature, these coefficients are not considered random anymore. We describe an interscale orthonormal wavelet thresholding algorithm based on this new approach and show its near-optimal performance—both regarding quality and CPU requirement—by comparing it with the results of three state-of-the-art nonredundant denoising algorithms on a large set of test images. An interesting fallout of this study is the development of a new, group-delay-based,parent–child prediction in a wavelet dyadic tree.

V A NON-LOCAL ALGORITHM[7]

In this study they propose a new measure, the method noise, to evaluate and compare the performance of digital image denoising methods. We first compute and analyze this method noise for a wide class of denoising algorithms, namely the local smoothing filters. Second, we propose a new algorithm, the non-local means (NL-means), based on a non-local averaging of all pixels in the image. present some experiments comparing the NL-means algorithm and the local smoothing filters. Several methods have been proposed to remove the noise and recover the true image u. Even though they may be very different in tools it must be emphasized that a wide class share the same basic remark : denoising is achieved by averaging. This averaging may be performed locally: the Gaussian smoothing model the anisotropic filtering and the neighborhood filtering by the calculus of variations: the Total Variation minimization or in the frequency domain: the empirical Wiener filters and wavelet thresholding methods.

A New SURE Approach to Image Denoising[4]

This paper introduces a new approach to orthonormal wavelet image denoising. Instead of postulating a statistical model for the wavelet coefficients, we directly parametrize the denoising process as a sum of elementary nonlinear processes with unknown weights.We then minimize an estimate of the mean square error between the clean image and the denoised one. The key point is that we have at our disposal a very accurate, statistically unbiased, MSE estimate—Stein's unbiased risk estimate that depends on the noisy image alone, not on the clean one. Like the MSE, this estimate is quadratic in the unknown weights, and its minimization amounts to solving a linear system of equations. The existence of this *a priori* estimate makes it unnecessary to devise a specific statistical model for the wavelet coefficients. Instead, and contrary to the custom in the literature, these coefficients are not considered random anymore. We describe an interscale orthonormal wavelet thresholding algorithm based on this new approach and show its near-optimal performance—both regarding quality and CPU requirement—by comparing it with the results of three state-of-the-art nonredundant denoising algorithms on a large set of test images. An interesting fallout of this study is the development of a new, group-delay-based,parent–child prediction in a wavelet dyadic tree.

Image Denoising Via Sparse and Redundant Representations[6]

This study gives the image denoising problem, where zero-mean white and homogeneous Gaussian additive noise is to be removed from a given image. The approach taken is based on sparse and redundant representations over trained dictionaries. Using the K-SVD algorithm, we obtain a dictionary that describes the image content effectively. Two training options are considered: using the corrupted image itself, or training on a corpus of high-quality image database. Since the K-SVD is limited in handling small image patches, we extend its deployment to arbitrary image sizes by defining a global image prior that forces sparsity over patches in every location in the image.We show how such Bayesian treatment leads to a simple and effective denoising algorithm. This leads to a state-of-the-art denoising performance, equivalent and sometimes surpassing recently published leadingalternative denoising methods. This work has presented a simple method for image denoising, leading to state-of-the-art performance, equivalent to and sometimes surpassing recently published leading alternatives. The proposed method is based on local operations and involves sparse decompositions of each image block under one fixed over-complete dictionary, and a simple average calculations. The content of the dictionary is of prime importance for the denoising process—we have shown that a dictionary trained for natural real images, as well as an adaptive dictionary trained on patches of the noisy image itself, both perform very well.

Image denoising by sparse 3D transform-domain collaborative filtering[9]

This study proposes a novel image denoising strategy based on an enhanced sparse representation in transform domain. The enhancement of the sparsity is achieved by grouping similar 2-D image fragments into 3-D data arrays which we call "groups." Collaborative filtering is a special procedure developed to deal with these 3-D groups. We realize it using the three successive steps: 3-D transformation of a group, shrinkage of the transform spectrum, and

inverse 3-D transformation. The result is a 3-D estimate that consists of the jointly filtered grouped image blocks. By attenuating the noise, the collaborative filtering reveals even the finest details shared by grouped blocks and, at the same time, it preserves the essential unique features of each individual block. The filtered blocks are then returned to their original positions. Because these blocks are overlapping, for each pixel, we obtain many different estimates which need to be combined. Aggregation is a particular averaging procedure which is exploited to take advantage of this redundancy. A significant improvement is obtained by a specially developed collaborative Wiener filtering. An algorithm based on this novel denoising strategy and their efficient implementations are presented in full detail; an extension to color-image denoising is also developed. The experimental results demonstrate that this computationally scalable algorithm achieves state-of-the-art denoising performance in terms of both peak signal-to-noise ratio and subjective visual quality.

Noise removal using smoothed normals and surface fitting

In this work, we use partial differential equation techniques to remove noise from digital images. The removal is done in two steps. We first use a total-variation filter to smooth the normal vectors of the level curves of a noise image. After this, we try to find a surface to fit the smoothed normal vectors. For each of these two stages, the problem is reduced to a nonlinear partial differential equation. Finite difference schemes are used to solve these equations. A broad range of numerical examples are given in the paper. In this paper, they tried to process three dimensional surfaces. The essential idea was to manipulate the normal vectors for a given three dimensional surface and then find a new surface that matches the processed normal vectors in a suitable way. In this work, we are extending the idea of to do image noise removal. Further, we would like to mention that normal processing has also been used in shape from shading reconstruction and in mesh optimization

VI THE CURVELET TRANSFORM FOR IMAGE DENOISING,[11]

This study describe approximate digital implementations of two new mathematical transforms, namely, the ridgelet transformand the curvelet transform. Our implementationsoffer exact reconstruction, stability against perturbations, ease of implementation, and low computational complexity. A central tool is Fourier-domain computation of an approximate digital Radon transform. We introduce a very simple interpolation in Fourier space which takes Cartesian samples and yields samples on a rectopolar grid, which is a pseudo-polar sampling set based on a concentric squares geometry. Despite the crudeness of ourinterpolation, the visual performance is surprisingly good. Our ridgelet transform applies to the Radon transform a special overcomplete wavelet pyramid whose wavelets have compactsupport in the frequency domain. Our curvelet transform uses our ridgelet transform as a component step, and implements curvelet subbands using a filter bank of à trous wavelet filters. Our philosophy throughout is that transforms should be over complete, rather than critically sampled. We apply these digital transforms to the denoising of some standard images embedded in white noise. In the tests reported here, simple thresholding of the

International Journal of Electrical and Electronics Engineers
Vol. No. 8, Issue No. 02, July-December 2016
ISSN (O) 2321-2055
ISSN (P) 2321-2045

curvelet coefficients is very competitive with "state of the art" techniques based on wavelets, including thresholding of decimated or undecimated wavelet transforms and also including tree-based Bayesian posterior mean methods. Moreover, the curvelet reconstructions exhibit higher perceptual quality than wavelet-based reconstructions, offering visually sharper images and, in particular, higher quality recovery of edges and of faint linear and curvilinear features. Existing theory for curvelet and ridgelet transforms suggests that these new approaches can outperform wavelet methods in certain image reconstruction problems. The empirical results reported here are in encouraging agreement.

VII A DECOMPOSITION FRAMEWORK FOR IMAGE DENOISING ALGORITHMS[1]

In this study gives an imagedecomposition model that provides a novel framework for image denoising. The model computes the components of the image to be processedin a moving frame that encodes its local geometry (directions of gradients and level lines). Then, the strategy we develop is to denoise the components of the image in the moving frame in order to preserve its local geometry, which would have been more affected if processing the image directly. Experiments on a whole image database tested with several denoising methods show that this framework can provide better results than denoising the image directly, both in terms of Peak signal-to-noise ratio and Structural similarity index metrics.

System Block Diagram of Image Denoising

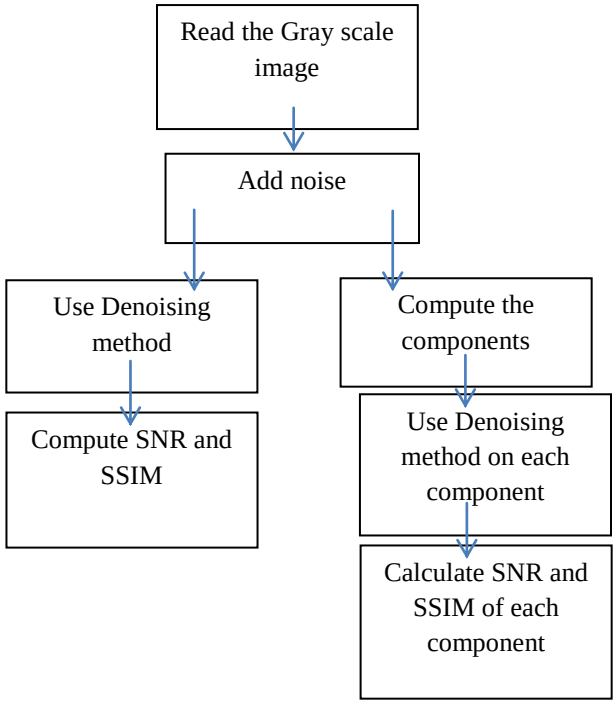

International Journal of Electrical and Electronics Engineers
Vol. No. 8, Issue No. 02, July-December 2016
ISSN (O) 2321-2055
ISSN (P) 2321-2045

FIG: BLOCK DIAGRAM OF IMAGE DENOISING METHOD

The flow of proposed work is to compute the components of the image, then these components will be denoised which preserves the local geometry of images like edges, gray level gradient etc. Thus improving the Peak signal-to-noise ratio and Structural similarity index metrics, we get better denoised image

7.1 The Gray-Level Case

Let I:⊂R2 → R be a gray-level image, and (x, y) be the standard coordinate system of R2. We denote by Ix resp. Iy the derivative of I with respect to x resp. y, and by ∇I the gradient of I. Our image decomposition model for I is a two-stages approach:

First, we construct an orthonormal moving frame (Z1, Z2, N) of (R3,__2) over _ that encodes the local geometry of I . Then, we compute the components (J 1, J 2, J 3) of the R3-valued function (0, 0, I) in that moving frame. More precisely, we consider a scaled version μI of I , for μ ∈]0, 1], and its graph, which is the surface S in R3 parameterized by

ψ : (x, y) --→ (x, y,μ I (x, y)) (1)

The orthonormal moving frame (Z1, Z2, N) we consider is the following: the vector field Z1 is tangent to the surface S and indicates the direction of the steepest slope at each point of S; the vector field Z2 is tangent to S and indicates the direction of the lowest slope at each point of S. It follows that N is normal to the surface since we require (Z1, Z2, N) to be orthonormal. The moving frame (Z1, Z2, N) can be constructed as follows. Let z1 = (μIx,μIy)T be the gradient of μI and z2 = (−μIy,μIx)T indicating the direction of the level-lines of μI . On homogeneous regions of I , i.e. at pixel locations (x, y) where Ix (x, y) = Iy (x, y) = 0, we define z1 = (1, 0)T and z2 = (0, 1)T . Then, Z1 and Z2 are given by the following expressions

$$Zi = d\psi(zi)/lld\psi(zi)ll2 \quad , i = 1,2 \qquad (2)$$

where dψ stands for the differential of ψ, which maps vector fields on _ to tangent vector fields of S. The expression of the unit normal N is then obtained as the vectorial product between Z1 and Z2.The explicit expressions of the vector fields **Z1, Z2, N** are given by the matrix field

$$P = \begin{pmatrix} \frac{I_x}{\sqrt{|\nabla I|^2(1+\mu^2|\nabla I|^2)}} & \frac{-I_y}{|\nabla I|} & \frac{-\mu I_x}{\sqrt{1+\mu^2|\nabla I|^2}} \\ \frac{I_y}{\sqrt{|\nabla I|^2(1+\mu^2|\nabla I|^2)}} & \frac{I_x}{|\nabla I|} & \frac{-\mu I_y}{\sqrt{1+\mu^2|\nabla I|^2}} \\ \frac{\mu|\nabla I|^2}{\sqrt{|\nabla I|^2(1+\mu^2|\nabla I|^2)}} & 0 & \frac{1}{\sqrt{1+\mu^2|\nabla I|^2}} \end{pmatrix}, \qquad (3)$$

International Journal of Electrical and Electronics Engineers
Vol. No. 8, Issue No. 02, July-December 2016
ISSN (O) 2321-2055
ISSN (P) 2321-2045

where the coordinates of the vector field **Z1** are given in the first column, the coordinates of **Z2** in the second column, and the coordinates of **N** in the third column.

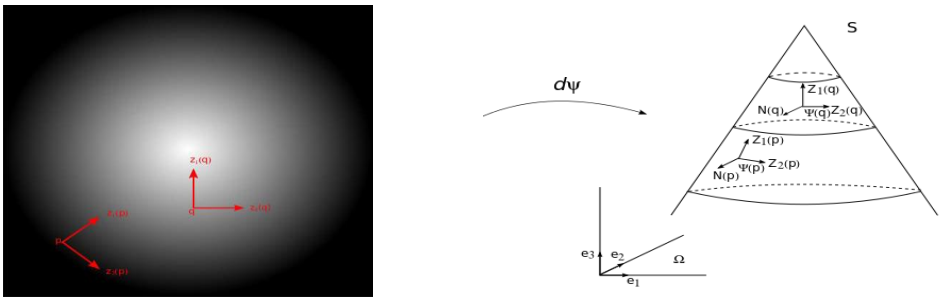

Fig. 1 illustrates the moving frames (z1, z2) and (Z1, Z2, N) aforementioned for a simple image. The left image shows the moving frame (z1, z2) at two points p and q of the domain and the right image shows the induced moving frame (Z1, Z2, N) attached to the surface S at the points ψ(p) and ψ(q).

Fig. 1 illustrates the moving frames (z1, z2) and(Z1, Z2, N) aforementioned for a simple image. The left image shows the moving frame (z1, z2) at two points p and q of the domain, and the right image shows the inducedmoving frame (Z1, Z2, N) attached to the surface S at thepoints ψ(p) and ψ(q). Denoting by (e1, e2, e3) the orthonormal frame of (R3,__2), where e1 = (1, 0, 0), e2 = (0, 1, 0), e3 = (0, 0, 1), the matrix P in (3) is nothing but the frame change field from (e1, e2, e3) to (Z1, Z2, N), meaning that the components of the R3-valued function (0, 0, I) in the new frame, denoted by (J 1, J 2, J 3), are given by

$$\begin{pmatrix} J^1 \\ J^2 \\ J^3 \end{pmatrix} = P^{-1} \begin{pmatrix} 0 \\ 0 \\ I \end{pmatrix}. \qquad (4)$$

7.2 The Multi-Channel Case

We aim at extending the image decomposition model of Sect. II.A from gray-level to n-channel images I =(I 1, · · · , I n) : _ ⊂R2 −→ Rn, n >1, by following a similar approach: first, we construct an orthonormal moving frame **(Z1, Z2, N1, · · · , Nn)** of (Rn+2,__2) over _ that encodes the local geometry of I . Then, we compute the components (J 1, J 2, · · · , J n+2) of the Rn+2-valued function (0, 0, I 1, · · · , I n) in that moving frame. As in the gray-level case, the first step consists in considering a scaled version μI of I, for μ ∈]0, 1], and its graph, which is the surface S in Rn+2 parametrized by

$$\psi : (x, y) \longrightarrow (x, y, \mu I^1(x, y), \cdots, \mu I^n(x, y)) \qquad (5)$$

The moving frame **(Z1, Z2, N1, · · · , Nn)** we consider is then the following: the vector field **Z1** is tangent to the surface S and indicates the direction of the steepest slope at each point of S; the vector field **Z2** is tangent to S and

International Journal of Electrical and Electronics Engineers
Vol. No. 8, Issue No. 02, July-December 2016
ISSN (O) 2321-2055
ISSN (P) 2321-2045

indicates the direction of the lowest slope at each point of S, and **N1, · · · , Nn** are normals to the surface. Note that, unlike the gray-level case, there is an infinite number of unit normals to the surface.

The moving frame **(Z1, Z2, N1, · · · , Nn)** can be constructed as follows. As in the gray-level case, **Z1** and **Z2** can be recovered from the directions **z1** and **z2** of highest and lowest variations of the scaled image μI under the map (2), these latter being the eigenvectors of the structure tensor associated to μI , which is given by

$$\begin{pmatrix} \sum_{k=1}^{n} (\mu I_x^k)^2 & \sum_{k=1}^{n} \mu^2 I_x^k I_y^k \\ \sum_{k=1}^{n} \mu^2 I_x^k I_y^k & \sum_{k=1}^{n} (\mu I_y^k)^2 \end{pmatrix} \qquad (6)$$

On homogeneous regions, i.e. at pixel locations (x, y) where $I_x^k(x,y) = I_y^k(x,y) = 0 \ \forall k \in \{1, \cdots, n\}$, we set $z_1 = (1,0)^T$. It is worth noting that, unlike gray-level images, multi-channel images do not have necessarily levellines, meaning that the smallest eigenvalues of the structure tensor are not necessarily 0. We then need to select a set of n vector fields **N1, · · · , Nn** normal to the surface and orthogonal to each other in order to complete the orthonormal moving frame. A natural approach for constructing them is to consider the canonical vectors

e3 = (0, 0, 1, 0, · · · , 0), · · · , **en+2** = (0, · · · , 0, 1) from which we apply the Gram-Schmidt orthonormalization process to the frame field **(Z1, Z2, e3, · · · , en+2)**.

Finally, denoting by P the matrix field encoding the moving frame **(Z1, Z2, N1, · · · , Nn)**, i.e. the first column of P contains the coordinates of Z1, the second column the coordinates of Z2, and the i -th column the coordinates of Ni−2 for i ∈ {3, · · · , n + 2}, the components (J 1, · · · , J n+2) of the Rn+2-valued function (0, 0, I 1, · · · , I n) in the frame

(Z1, Z2, N1, · · · , Nn) are given by

$$\begin{pmatrix} J^1 \\ J^2 \\ J^3 \\ \vdots \\ J^{n+2} \end{pmatrix} = P^{-1} \begin{pmatrix} 0 \\ 0 \\ I^1 \\ \vdots \\ I^n \end{pmatrix} \qquad (7)$$

Unlike the gray-level case, it is not possible to plot the moving frame in a trivial way since the surface S lives in a space of dimension greater than or equal to 4.

7.3 Application to Image Denoising

The framework we propose for denoising an image while systematically taking into account its local geometry is based on applying image denoising techniques to the componentsof the image in the moving frame constructed

International Journal of Electrical and Electronics Engineers
Vol. No. 8, Issue No. 02, July-December 2016
ISSN (O) 2321-2055
ISSN (P) 2321-2045

above instead of applying the technique to the image itself. This methodology has already been used in [2]–[4] with local regularization/denoising methods, but it can actually be extended to any denoising technique. In this section, we give more details about our approach dealing with gray-level and color images.

7.3.1 Gray-Level Images: In the experiments performed throughout this article, the strategy on gray-level images I : _ ⊂R2 −→ R is the following:

1) Process I with some denoising technique F and call the output image Iden.

2) Compute the components (J 1, J 2, J 3) of I in the moving frame (3), for some scalar μ, with formula (4). Apply the same denoising technique F to the components to obtain the processed components (J 1 den, J 2 den, J 3 den). Then, apply the inverse frame change matrix field to the processed components, i.e.

$$\begin{pmatrix} I^1_{denMF} \\ I^2_{denMF} \\ I^3_{denMF} \end{pmatrix} := P \begin{pmatrix} J^1_{den} \\ J^2_{den} \\ J^3_{den} \end{pmatrix} \qquad (8)$$

and denote by IdenMF the third component I 3 denMF.

1) Compare Iden and IdenMF with the metrics PSNR and SSIM.

7.3.2 Color Images: The extension to color images is not straightforward because of the flexibility of the choice of color space and the way in which the moving frame approach

can be applied (channel-wise, only to selected channels, or vectorially). We will see in the next two sections that the color space and manner in which the approach is applied both depend on the image denoising technique. However, in all of the experiments performed throughout this article, our approach for color images I : _ ⊂R2 −→ R3 is of the form:

1) Process I with an image denoising technique F and call the output image Iden.

2) Apply the same image denoising technique F to the components in some moving frame related to the channels of the image or the full image itself. Then apply the inverse frame change matrix field to the processed components, from which a color image IdenMV is reconstructed.

3) Compare Iden and IdenMV with the metrics PSNR and SSIM. Note that SSIM has been originally designed for gray-level images, and we define the SSIM Index for color images as the mean of the SSIM Index of each color channel. Finally, we would like to point out that the strategy described above can actually be applied using any moving frame.

VIII CONCLUSION

In this proposed work, we have to develop a framework that enables any denoising method to take more into account the local geometry of the image to be denoised by preserving the moving frame describing the graph of a scaled version of the image. Experiments with the VTV-based denoising method, NLM and BM3D algorithms on both gray-level and color images tested over the Kodak database showed that our strategy systematically improves the denoising method it is applied to, in terms of PSNR and SSIM metrics. The fact that we have been able to improve the performance of three denoising methods of different types: a local variational method, a patch-based method, and a method combining a patch based approach with a filtering in spectral domain approach, demonstrates the consistency of our methodology.However, as the components have different geometric meaning, one shall wonder whether they should not rather be denoised with different denoising methods, and we are currently investigating that point.

REFERENCES

[1]Gabriela Ghimpe¸teanu, Thomas Batard, Marcelo Bertalmío, and Stacey Levine, "A Decomposition Framework for Image Denoising Algorithms," in Proc.IEEE Transactions on image processing, vol. 25, no. 1, january 2016

[2] S. P. Awate and R. T. Whitaker, "Higher-order image statistics for unsupervised,information-theoretic, adaptive, image filtering," in Proc.IEEE Comput. Soc. Conf. Comput. Vis. Pattern Recognit., vol. 2. Jun. 2005, pp. 44–51.

[3] T. Batard and M. Berthier, "Spinor Fourier transform for image processing," IEEE J. Sel. Topics Signal Process., vol. 7, no. 4, pp. 605–613, Aug. 2013.

[4] Florian Luisier, Thierry Blu, and Michael Unser, "A New SURE Approach to Image Denoising: Interscale Orthonormal Wavelet Thresholding," in *IEEE Trans. Image Process.*, vol. 15, no. 3, pp. 645–665, Mar. 2006.

[5] P. Blomgren and T. F. Chan, "Color TV: Total variation methods for restoration of vector-valued images," IEEE Trans. Image Process, vol. 7, no. 3, pp. 304–309, Mar. 1998.

[6] X. Bresson and T. F. Chan, "Image Denoising Via Sparse and Redundant Representations Over Learned Dictionaries" InverseProblems Imag., vol. 2, no. 4, pp.455–484, 2008.

[7] A. Buades, B. Coll, and J.-M. Morel, "A non-local algorithm for image denoising," in Proc. IEEE Comput. Soc. Conf. Comput. Vis. PatternRecognit., vol. 2. Jun. 2005, pp. 60–65.

[10] M. Lysaker, S. Osher, and X.-C. Tai, "Noise removal using smoothed normals and surface fitting," *IEEE Trans. Image Process.*, vol. 13, no. 10, pp. 1345–1357, Oct2004

[9] K. Dabov, A. Foi, V. Katkovnik, and K. Egiazarian, "Image denoising by sparse 3D transform-domain collaborative filtering," IEEE Trans. ImageProcess., vol. 16, no. 8, pp. 2080–2095, Aug. 2007.

[10] Z. Wang, A. C. Bovik, H. R. Sheikh, and E. P. Simoncelli, "Image quality assessment: From error visibility to structural similarity," *IEEETrans. Image Process.*, vol. 13, no. 4, pp. 600–612, Apr. 2004.

[11] Jean-Luc Starck, Emmanuel J. Candès, and David L. Donoho, "The Curvelet Transform for Image Denoising," *IEEETrans. Image Process.*, vol. 11, no. 6, pp. 600–612, june 2012.